Sympathetic Dysfunction in Type 1 Diabetes

Association With Impaired Myocardial Blood Flow Reserve and Diastolic Dysfunction

Rodica Pop-Busui, MD,*§ Ian Kirkwood, MBBS,* Helena Schmid, MD,* Victor Marinescu, BS,*
Justin Schroeder, BS,* Dennis Larkin, BS,* Elina Yamada, MD,† David M. Raffel, PhD,‡
Martin J. Stevens, MD*

Ann Arbor, Michigan; and Toledo, Ohio

OBJECTIVES	This study was designed to explore the relationships of early diabetic microangiopathy to alterations of cardiac sympathetic tone and myocardial blood flow (MBF) regulation in subjects with stable type 1 diabetes.
BACKGROUND	In diabetes, augmented cardiac sympathetic tone and abnormal MBF regulation may predispose to myocardial injury and enhanced cardiac risk.
METHODS	Subject groups comprised healthy controls (C) (n = 10), healthy diabetic subjects (DC) (n = 12), and diabetic subjects with very early diabetic microangiopathy (DMA+) (n = 16). [^{11}C]*meta*-hydroxyephedrine ([^{11}C]HED) and positron emission tomography (PET) were used to explore left ventricular (LV) sympathetic integrity and [^{13}N]ammonia-PET to assess MBF regulation in response to cold pressor testing (CPT) and adenosine infusion.
RESULTS	Deficits of LV [^{11}C]HED retention were extensive and global in the DMA+ subjects (36 ± 31% vs. 1 ± 1% in DC subjects; p < 0.01) despite preserved autonomic reflex tests. On CPT, plasma norepinephrine excursions were two-fold greater than in C and DC subjects (p < 0.05), and basal LV blood flow decreased (−12%, p < 0.05) in DMA+ but not in C or DC subjects (+45% and +51%, respectively). On adenosine infusion, compared with C subjects, MBF reserve decreased by ~45% (p < 0.05) in DMA+ subjects. Diastolic dysfunction was detected by two-dimensional echocardiography in 5 of 8 and 0 of 8 consecutively tested DMA+ and DC subjects, respectively.
CONCLUSIONS	Augmented cardiac sympathetic tone and responsiveness and impaired myocardial perfusion may contribute to myocardial injury in diabetes. (J Am Coll Cardiol 2004;44:2368–74) © 2004 by the American College of Cardiology Foundation

In diabetes, the etiology of enhanced cardiac risk is thought to reflect the detrimental consequences of myocardial ischemia, oxidative stress, and alterations in myocardial substrate metabolism (1–3). Additionally, a putative diabetic cardiomyopathy comprising myocardial interstitial and perivascular fibrosis (1) and apoptosis (2) has been identified in patients without coronary artery disease and linked to the development of impaired left ventricular (LV) function (3). Indeed, alterations of diastolic (3–5) and systolic (6) function are widely reported in healthy diabetic subjects and often predate the development of other chronic diabetic complications.

Although the etiology of myocardial injury and dysfunction in diabetes uncomplicated by the presence of coronary vascular disease is not well understood, alterations of cardiac sympathetic innervation, tone, and responsiveness (7,8), coupled with abnormal myocardial blood flow (MBF) regulation (9–14), have emerged as potential contributing factors. In experimental diabetes, the initial development of cardiovascular autonomic neuropathy (CAN) is characterized by early augmentation of sympathetic tone (15,16), which may contribute to myocardial injury (15,17). Therefore, in diabetes, increased cardiac sympathetic nervous system activity and elevated cardiac synaptic norepinephrine (15,18) or enhanced myocardial norepinephrine sensitivity may provide a mechanistic explanation for myocardial injury predisposing to the development of impaired LV function and enhanced cardiac risk. We therefore wished to explore the hypothesis that early preclinical diabetic microangiopathy is complicated by abnormalities in cardiac sympathetic nervous system innervation and blood flow regulation, which could ultimately predispose to the development of cardiomyopathy.

METHODS

Patient population. Subjects with type 1 diabetes were recruited from the Michigan Diabetes Research and Training Center. Subject groups comprised healthy nondiabetic

---

Abbreviations and Acronyms

C	=	controls
CAN	=	cardiovascular autonomic neuropathy
CPT	=	cold pressor testing
CRP	=	C-reactive peptide
DC	=	diabetic control subjects
DMA+	=	early microangiopathy
LV	=	left ventricle/ventricular
MBF	=	myocardial blood flow
PET	=	positron emission tomography
vWF	=	von Willebrand factor
([^{11}C]HED)	=	[^{11}C]*meta*-hydroxyephedrine

---

controls (C) (n = 10); healthy diabetic control subjects (DC) (n = 12); and diabetic subjects with very early microangiopathy (DMA+) (n = 16), defined by the presence of early nonproliferative diabetic retinopathy (n = 14) or early microalbuminuria (n = 2) and/or early peripheral neuropathy (n = 10). All subjects were matched for age and diabetes duration and were free from dyslipidemia and macrovascular complications (Table 1).

All of the DMA+ subjects had undergone negative scintigraphic cardiac stress testing within one year preceding this study. No subjects had a history of hypertension or were taking vasoactive medications, lipid-lowering agents, or medications known to alter sympathetic tone. Written informed consent was obtained and the study protocol was approved by the institutional review board of the University of Michigan.

Criteria for retinopathy and nephropathy. Retinopathy was graded by stereoscopic color photographs using the Early Treatment of Diabetic Retinopathy Scale (EDTRS) (19). The DC subjects were without retinopathy (level 10). Level 20 of the EDTRS was divided into two subgroups: level 20a, with ≥1 and <3 microaneurysms, and level 20b, with ≥3 microaneurysms. The DMA+ subjects were de-

Table 1. Clinical Details

	C (n = 10)	DC (n = 12)	DMA+ (n = 16)
Male:female	6:4	7:5	11:5
Age (yrs)	38 ± 8	43 ± 9	41 ± 10
Diabetes duration (yrs)	—	28 ± 7	21 ± 11
Hb A$_{1c}$	4.8 ± 0.2	7.8 ± 1.1*	7.8 ± 1.3*
Urinary microalbuminuria (>30 mg/24 h) (−/+)	N/D	12/0	14/2
MNSI questionnaire (−/+)	N/D	12/0	6/10
MNSI examination (−/+)	N/D	12/0	16/0
Retinopathy (level 10/levels 20b–35/proliferative)	N/D	12/—/—	—/16/—
Total cholesterol (mg/dl)	191 ± 59	191 ± 43	165 ± 34
LDLc (mg/dl)	107 ± 48	120 ± 43	90 ± 27
HDLc (mg/dl)	57 ± 16	53 ± 20	54 ± 19
Triglycerides (mg/dl)	119 ± 74	94 ± 62	110 ± 52

Data shown as mean values ± SD. *p < 0.05 vs. C.
C = controls; DC = diabetic control subjects; DMA+ = early microangiography; Hb = hemoglobin; HDLC = high-density lipoprotein cholesterol; LDLC = low-density lipoprotein cholesterol; MNSI = Michigan Neuropathy Screening Instrument; N/D = not done.

Table 2. Autonomic Neuropathy Details

	C	DC	DMA+
Heart rate variability (beats/min)	21 ± 8	20 ± 5	18 ± 12
Valsalva ratio	1.57 ± 0.3	1.58 ± 0.4	1.61 ± 0.37
30/15 ratio	1.38 ± 0.2	1.17 ± 0.07	1.25 ± 0.2
Systolic BP response to standing (mm Hg)	+12 ± 5	+2 ± 6	−3 ± 7

Data shown as mean values ± SD.
BP = blood pressure; other abbreviations as in Table 1.

fined by level 20b to 35 retinopathy or microalbuminuria (20).

CRITERIA FOR NEUROPATHY. Subjects were classified for neuropathy based on the results of cardiovascular autonomic function testing (21) (Table 2) and the Michigan Neuropathy Screening Instrument (MNSI) examination score (22). The DC subjects had no evidence of neuropathy; DMA+ had no or minimal evidence of neuropathy (<2 abnormal CAN reflex tests, normal MNSI examination score, normal or abnormal MNSI symptom score).

Positron emission tomography (PET) studies. Cardiac PET imaging was performed with a whole-body PET scanner (Siemens ECAT/931, Siemens/ECAT Exact, or Siemens/ECAT Exact HR+, Siemens Medical Solutions, Malvern, Pennsylvania). There were three separate PET imaging sessions. The first session used [^{11}C]*meta*-hydroxyephedrine ([^{11}C]HED) to evaluate the integrity of cardiac sympathetic innervation. The second session used [^{13}N]ammonia to measure MBF regulation in response to cold pressor stimulation. The third session used [^{13}N]ammonia to measure the MBF reserve in response to adenosine infusion. All PET scans for a given patient were performed on the same scanner.

Evaluation of cardiac sympathetic innervation with [^{11}C]HED. After the transmission scan, a 60-min dynamic PET image acquisition sequence was started as 20 mCi of [^{11}C]HED was injected over 30 s, as previously reported (8). After correction for attenuation, transaxial PET data were reoriented and re-sliced into short-axis view data sets (slice thickness 0.8 cm) for subsequent quantitative analyses.

Regional neuronal retention of [^{11}C]HED was quantified using a "retention index" approach (8) that corrects for tracer delivery. The heterogeneity of regional LV [^{11}C]HED retention in each diabetic subject was compared with the normal reference distribution by performing a z-score analysis. Sectors that had a z score >2.5 were defined as abnormal. The extent of [^{11}C]HED retention heterogeneity was expressed as the percentage of all sectors in the patient's polar map that were abnormal (i.e., had z scores >2.5).

Evaluation of regional MBF regulation with [^{13}N]ammonia. [^{13}N]ammonia studies at rest and during stress were performed sequentially in a single session. The resting perfusion scan was started by initiating a 15-min dynamic PET acquisition sequence as 20 mCi of [^{13}N]ammonia was intravenously injected (9). After 50 min, a cold pressor stress

[¹³N]ammonia study was performed with stimulation starting 30 s before tracer injection. Blood pressure and heart rate were recorded at 1-min intervals. For the adenosine study, adenosine was infused intravenously over 6 min at 140 µg/kg/min to achieve maximal coronary vasodilatation (9). At 3 min, 20 mCi [¹³N]ammonia was injected over 30 s and imaged for 3 to 18 min. Blood pressure and heart rate were measured every minute during adenosine infusion and then at 10 and 18 min. Pressure-rate product was calculated as heart rate times systolic blood pressure divided by 100.

Regional MBF was estimated from the measured [¹³N]ammonia kinetics (23) as previously reported (9). Regional MBF reserve values were estimated by dividing the stress flow value by the resting flow value. Mean values of resting flow, stress flow, and MBF reserve were then determined for the same LV regions used in the [¹¹C]HED analysis.

Cold pressor testing (CPT). The CPT to provoke sympathetic activation was performed by applying a bag filled with ice chips to the forehead for 2 min (24).

Echocardiography. Two-dimensional echocardiography and pulsed tissue Doppler parameters were used to classify diastolic function (25). Data acquired included the ratio of peak flow velocities during early filling and atrial contraction (E/A ratio), Doppler tissue imaging of the mitral annulus early diastolic velocity (Ea), the mitral annular motion with atrial contraction (Aa), and the Doppler tissue imaging of the mitral annulus (Ea/Aa ratio). Left ventricular diastolic dysfunction was defined by an E/A ratio <1, or if >1, by an Ea/Aa ratio <1. Left ventricular mass was determined by the formula LV mass $= 0.8 \times 1.05 \times (S + P + LVEDD)3 - (LVEDD)3$, where S = LV septal thickness, P = LV posterior wall thickness, and LVEDD = LV end-diastolic diameter. The LV mass index was then determined (LV mass/body surface area). Abnormal LV mass index was defined by values ≥ 100 g/m² in women and ≥ 131 g/m² in men.

Oxidative stress measurements. Urine F2 isoprostanes were measured by enzyme-linked immunosorbent assay. Plasma total radical-trapping antioxidant parameter was measured as previously reported (26).

Statistical analysis. Statistical analysis was performed using Super ANOVA (Abacus Concepts Inc., Berkeley, California). The equality of experimental group means was tested by a one-way analysis of variance and, if significant, the differences were assessed by the Student-Newman-Keuls multiple-range test. If the variances for the variables differed significantly, logarithmic transformation was performed. All analyses were then performed on the transformed data. The significance of changes in measurements from baseline was determined using a paired *t* test. Significance was defined at the 0.05 level.

RESULTS

Glycemic control was equivalent in diabetic subjects (Table 1). The urine microalbumin/creatinine ratio was not significantly
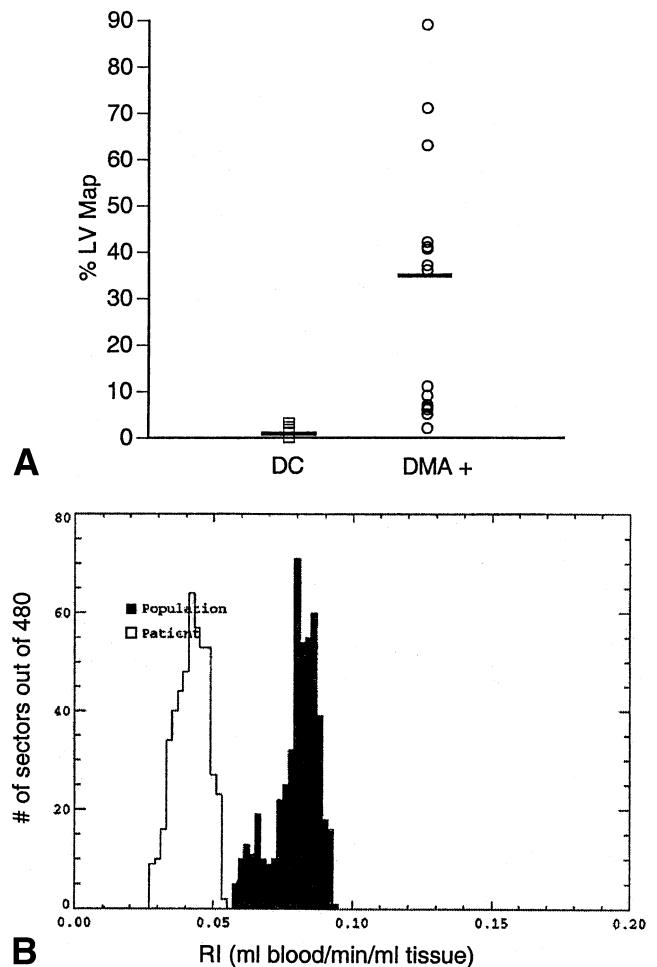
Figure 1. (A) Extent of left ventricular (LV) [¹¹C]*meta*-hydroxyephedrine ([¹¹C]HED) retention deficits in different subject groups. Normalized [¹¹C]HED retention data are displayed as polar coordinate maps of relative tracer activity ([¹¹C]/[¹³N]). The "extent" of the heterogeneity is expressed as the percentage of sectors in the polar map that are abnormal, i.e., $z_i > 2.5$. $p < 0.01$ early microangiopathy (DMA+) versus diabetic control subjects (DC). **Horizontal bars** = mean value. **(B)** Left ventricular [¹¹C]HED retention is globally decreased in a DMA+ subject. Quantitative assessment of LV [¹¹C]HED retention (expressed as a retention index [RI]) demonstrated reduced retention in all LV sectors in a DMA+ subject **(open plot)** compared with the values obtained in nondiabetic control subjects **(shaded plot)**.

different between DC and DMA+ subjects. Plasma lipid levels did not differ between groups. Ten DMA+ subjects either had symptoms consistent with peripheral neuropathy or one abnormal CAN reflect test (Table 2). However, none had an abnormal MNSI examination score.

DMA+ subjects demonstrate defects of LV[¹¹C]HED retention. Deficits of distal LV [¹¹C]HED retention affected <1% of the LV (Fig. 1A) in DC subjects, but affected ~36% of the LV in DMA+ subjects despite normal cardiovascular reflex testing. Unlike the small distal deficits of LV [¹¹C]HED retention identified in DC subjects, deficits of tracer retention in DMA+ subjects were more global, affecting both the basal as well as the distal segments (Fig. 1B).

Table 3. Heart Rate, BP, and Norepinephrine Response to CPT

	C	DC	DMA+
Heart rate, rest (beats/min)	56 ± 9	68 ± 10*	74 ± 16*
Heart rate, stress (beats/min)	67 ± 12	79 ± 13	86 ± 15*
Heart rate, delta (beats/min)	11 ± 7	13 ± 5	13 ± 7
Systolic BP, rest (mm Hg)	99 ± 17	121 ± 12*	128 ± 12*
Systolic BP, stress (mm Hg)	124 ± 30	154 ± 27	152 ± 17
Systolic BP, delta (mm Hg)	26 ± 15	29 ± 17	24 ± 14
Norepinephrine, rest (pg/ml)	312 ± 168	242 ± 96	228 ± 66
Norepinephrine, stress (pg/ml)	451 ± 245†	378 ± 89†	518 ± 200†
Norepinephrine, delta (pg/ml)	138 ± 37	135 ± 25	290 ± 85*

Data shown as mean value ± SD. *p < 0.05 vs. C. †p < 0.05 vs. baseline.
CPT = cold pressor testing; other abbreviation as in Tables 1 and 2.

Plasma norepinephrine excursions are exaggerated on CPT in DMA+ subjects. Resting heart rate and systolic blood pressure were higher in the diabetic subjects compared with controls (Table 3). Basal levels of plasma norepinephrine tended to be lower in all the diabetic subjects. On CPT, the change in norepinephrine levels was ~2-fold greater in DMA+ subjects than in the C and DC subjects (p < 0.05). No significant differences in resting or stress epinephrine levels were detected between groups (data not shown).

CPT results in paradoxical LV vasoconstriction in DMA+ subjects. In response to sympathetic activation, global MBF reserve was preserved in DC subjects and reduced by 35% (p < 0.05) in DMA+ subjects (Table 4). Regionally, in the basal myocardial segments, MBF reserve was preserved in DC subjects but very abnormal (a paradoxical 12% [p < 0.05] reduction of myocardial perfusion) in DMA+ subjects. Myocardial blood flow reserve in the distal myocardial segments paralleled global perfusion measurements, and reduced perfusion was not observed in DMA+ subjects.

Assessment for occult regional myocardial perfusion defects. Regional discrete perfusion defects were sought by visual and semiquantitative analysis of MBF at rest and during adenosine stress. Visual inspection of standardized color-coded blood flow images taken from the distal and

Table 4. LV MBF Reserve on CPT

Myocardial Region	C	DC	DMA+
Basal anterior	1.45 ± 0.59	1.51 ± 0.3	0.88 ± 0.22*
Distal inferolateral	1.6 ± 0.62	1.7 ± 0.4	0.99 ± 0.41*
Global	1.5 ± 0.49	1.47 ± 0.18	0.98 ± 0.15*

Data shown as mean values ± SD. *p < 0.05 vs. C and DC.
CPT = cold pressor testing; LV = left ventricular; MBF = myocardial blood flow; other abbreviations as in Table 1.
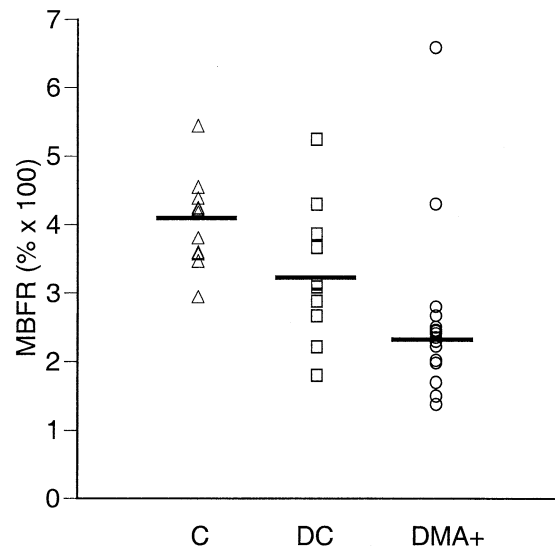
Figure 2. Change in global myocardial blood flow reserve (MBFR) in response to adenosine infusion. [^{13}N]ammonia positron emission tomography was used to explore MBF regulation in response to adenosine. p < 0.05 diabetic control subjects (DC) versus controls (C). p < 0.05 early microangiopathy (DMA+) versus C and DC. **Horizontal bars** = mean value.

basal short axis and the vertical and horizontal long axis confirmed homogeneous [^{13}N]ammonia retention.

Systemic hemodynamic responses to adenosine infusion. No differences were observed in the hemodynamic response to adenosine infusion among the subject groups. The resting and adenosine stress pressure-rate products were similar in the C and diabetic subjects (data not shown).

MBF reserve during adenosine stimulation is reduced in DMA+ subjects. Compared with C subjects (69 ± 9 ml/min/g of tissue), resting MBF was elevated in both the DC (85 ± 20 ml/100 g/min) and DMA+ (91 ± 13 ml/100 g/min) subjects (p < 0.05). During adenosine infusion, the increase in LV MBF was blunted in the DMA+ (204 ± 42 ml/100 g/min) compared with the DC (267 ± 126 ml/100 g/min) and C (275 ± 26 ml/100 g/min) subjects (p = 0.2). Finally, MBF reserve differed between groups (p < 0.01). Compared with C subjects, MBF reserve was reduced by 21% (p < 0.05) and 45% (p < 0.01) in the DC and DMA+ subjects, respectively (Fig. 2). The difference between DC and DMA+ subjects was also statistically significant (p < 0.05). In contrast to our previously reported findings in subjects with advanced CAN (9), LV MBF reserve did not differ regionally (data not shown).

Effect of diabetes and microangiopathy on von Willebrand factor (vWF) antigen, C-reactive peptide (CRP), and oxidative stress. Compared with C subjects (107 ± 60%), vWF antigen increased by 67% (p < 0.01) in DMA+ subjects (179 ± 54%) but was unchanged in DC subjects (115 ± 10%). In comparison with C subjects (0.05 ± 0.03 mg/dl), CRP levels increased by 1.8-fold (p = 0.4) and 4.2-fold (p < 0.05) in DC (0.09 ± 0.05 mg/dl) and DMA+ subjects (0.21 ± 0.2 mg/dl), respectively. Plasma total radical-trapping antioxidant parameter was decreased

Table 5. LV Diastolic Function

	DC (n = 8)	DMA+ (n = 8)	p Value
E-wave peak velocity (cm/s)	87 ± 19	74 ± 15	0.2
A-wave peak velocity (cm/s)	70 ± 20	80 ± 21	0.4
E/A ratio	1.27 ± 0.14	0.96 ± 0.21	0.008
Ea-wave peak velocity (cm/s)	26 ± 10	18 ± 5	0.09
Aa wave peak velocity (cm/s)	21 ± 8	23 ± 8	0.6
Ea/Aa ratio	1.25 ± 0.3	0.88 ± 0.3	0.06
LV mass index (g/m²)	80 ± 13	100 ± 32	0.2

Data shown as mean values ± SD.
A = peak velocity during atrial contraction; Aa = DTI of the mitral annulus with atrial contraction; E = peak velocity during early LV filling; Ea = DTI of the mitral annulus early diastolic velocity; LV = left ventricular; other abbreviations as in Table 1.

in all diabetic subjects (1,028 ± 44 µM, 754 ± 126 µM, and 547 ± 52 µM, in C, DC, and DMA+, respectively), with the difference between DMA+ and C subjects achieving statistical significance (p < 0.01). Compared with C subjects (99 ± 21 pg/mmol creatinine), urine 8-epi prostaglandin F2-alpha increased three-fold (278 ± 34 pg/mmol creatinine) (p = 0.4) and 11-fold (1,047 ± 247 pg/mmol creatinine) (p < 0.01) in DC and DMA+ subjects, respectively.

DMA+ subjects demonstrate LV diastolic dysfunction. Left ventricular function was assessed in consecutively recruited DMA+ (n = 8, mean age 50 ± 7 years, 5 men and 3 women) and DC (n = 8, mean age 44 ± 8 years, 4 men and 4 women) subjects who were within one year of completion of the other studies reported herein. No subject had abnormal systolic function. Six DMA+ subjects, but none of the DC subjects, exhibited diastolic dysfunction (Table 5). Three DMA+ subjects had an abnormal LV mass index, which was normal in all DC subjects.

DISCUSSION

The aim of this study was to explore the potential mechanisms linked to the development of enhanced cardiac risk in diabetes. Compared with healthy controls, diabetic subjects with early subclinical microangiopathy demonstrated extensive deficits of LV [11C]HED retention, exaggerated plasma norepinephrine excursions, impaired MBF regulation, and LV diastolic dysfunction. Therefore, we propose that in diabetes, augmented cardiac sympathetic tone and responsiveness in concert with impaired perfusion may contribute to the eventual development of myocardial injury.

The extensive global deficits of [11C]HED retention observed in DMA+ subjects despite good glycemic control differ markedly from previous findings in metabolically stable (8) or metabolically compromised (27) type 1 diabetic subjects, and they suggest an etiology other than neuronal loss or acute hyperglycemia-induced neuronal dysfunction. Moreover, these findings differ markedly from our previous findings in subjects with either early (28) or more severe (8,9) CAN (accompanied by abnormal CAN reflex tests), in whom deficits of [11C]HED retention begin distally and

then spread proximally and circumferentially, eventually resulting in islands of basal increased [11C]HED retention (8,9,28).

Sympathetic neurotransmitter analogues such as [11C]HED undergo highly specific and rapid uptake into sympathetic nerve varicosities via norepinephrine transporters ("uptake-1") (29). In the isolated rat heart elevated norepinephrine perfusion concentrations increase neuronal HED clearance rates, suggesting that neuronal "recycling" of HED is impaired by high synaptic norepinephrine levels (29). In the acute six-week diabetic rat heart, retention of LV [11C]HED is inversely related to increased cardiac norepinephrine levels (16), which precedes cardiac small nerve fiber loss (M.J. Stevens, personal observations, 1999). Moreover, an inverse relationship of myocardial retention of metaiodobenzyl guanidine to plasma catecholamines occurs in subjects with pheochromocytoma (30), which is thought to reflect competition for uptake into neuronal storage vesicles (31). These data implicate increased synaptic norepinephrine as the most likely explanation for the reduction of cardiac [11C]HED retention in DMA+ subjects. Direct measurement of cardiac norepinephrine spillover is, however, required to confirm the potential mechanism(s) of this defect.

In DMA+ subjects, systemic plasma norepinephrine excursions in response to CPT were exaggerated, consistent with enhanced cardiovascular sympathetic nervous system reactivity. The unchanged resting systemic plasma norepinephrine levels do not preclude an increase of basal cardiac adrenergic tone, as a similar disassociation has been identified in arrhythmogenic right ventricular cardiomyopathy, which is characterized by increased cardiac, but not systemic, sympathetic nerve activity (32). Although the mechanisms of increased norepinephrine responses in DMA+ subjects are unknown, depletion of nitric oxide (and hence dysinhibition) in sympathetic ganglia (33) and/or vascular endothelium (34) or vascular denervation (35) have been proposed. It is unclear as to whether cardiac norepinephrine responsiveness was increased in parallel. More detailed determination of systemic and regional norepinephrine kinetics in DMA+ subjects is required to confirm and extend these observations.

In DMA+ subjects, increased adrenergic reactivity was associated with increased oxidative stress, elevated CRP and plasma vWF antigen, and impaired MBF reserve, consistent with endothelial dysfunction. On CPT, however, the most abnormal blood flow responses were observed in the basal myocardial segments. Diabetes-induced endothelial dysfunction is expected to be global in the LV, suggesting that other factors such as variations in the density of LV sympathetic innervation may have contributed (16). These findings are consistent with our earlier identification of maximal impairment of MBF reserve in the innervated basal myocardium of diabetic subjects with advanced CAN (9). On sympathetic activation, augmented accumulation of norepinephrine, increased oxidative stress, and apoptosis (36) may have

contributed to abnormal vascular reactivity. Paradoxic vasoconstriction responses (10,11,37) complicate coronary atherosclerosis. Our studies indicate that paradoxic coronary vasoconstriction can occur in type 1 diabetes in the absence of atheroma. (Alternatively, however, we cannot exclude the less likely possibility that globally impaired cardiac sympathetic function was principally the cause of the blunted MBF response.)

On adenosine infusion, global MBF reserve was reduced in DMA+ subjects to an extent that exceeded that observed in the DC subjects. Reduced MBF reserve has been reported in subjects with type 2 diabetes (11,12) as well as type 1 diabetes (9,12–14) and has been associated with impaired glucose control (38) or cardiovascular sympathetic denervation (9,14). We have now demonstrated that neither impairment of metabolic control nor the presence of cardiovascular denervation is a prerequisite for the development of impaired vasodilatory reserve. Although the mechanism(s) of this deficit is unknown, endothelial dysfunction, in concert with decreased myocardial vascularity (9,39), may be an important contributing factor.

In diabetes, a putative cardiomyopathy comprising myocardial interstitial and perivascular fibrosis (1) and apoptosis (2) has been linked to impaired LV function (3). Our preliminary studies identified diastolic dysfunction in five of eight consecutively recruited DMA+ subjects but none of the healthy DC subjects. Although the precise pathogenetic mechanisms are unclear, alterations of sympathetic tone could contribute to myocardial damage. For example, increased cardiac sympathetic tone may decrease myocardial vascularity (39), stimulate vascular hyperreactivity (40), increase mitochondrial reactive oxygen species production (17), perturb intracellular signaling (41), precipitate myocardial apoptosis (2,41), and promote myocardial remodeling (42). Therefore, in the course of the development of the microvascular complications of diabetes, elevated cardiac sympathetic tone may play a key pathogenetic role in the subsequent development of myocardial injury and dysfunction.

Conclusions. In summary, subjects with stable type 1 diabetes and preclinical microangiopathy demonstrate wide-ranging abnormalities of cardiac sympathetic innervation and blood flow regulation, which may contribute to the subsequent development of myocardial injury. Limitations of our study include the relatively small subject number as well as the cross-sectional design, which, although it provides provocative new findings, does not directly address the role of these pathophysiologic changes in the development of impaired myocardial function. Future larger, prospective studies are needed to confirm these preliminary observations. Direct confirmation of the findings presented herein may form the rationale for the development of prophylactic treatment strategies aimed at reducing cardiac risk in diabetes.

Reprint requests and correspondence: Dr. Martin J. Stevens, Division of Endocrinology and Metabolism, Department of Internal Medicine, University of Michigan, 5570 MSRB II, Box 0678, 1150 West Medical Center Drive, Ann Arbor, Michigan 48109-0678. E-mail: stevensm@umich.edu.

REFERENCES

1. Francis GS. Diabetic cardiomyopathy: fact or fiction? Heart 2001;85:247–8.
2. Frustaci A, Kajstura J, Chimenti C, et al. Myocardial cell death in human diabetes. Circ Res 2000;87:1123–32.
3. Fang ZY, Yuda S, Anderson V, Short L, Case C, Marwick TH. Echocardiographic detection of early diabetic myocardial disease. J Am Coll Cardiol 2003;41:611–7.
4. Kahn JK, Zola B, Juni JE, Vinik AI. Radionuclide assessment of left ventricular diastolic filling in diabetes mellitus with and without cardiac autonomic neuropathy. J Am Coll Cardiol 1986;7:1303–9.
5. Zarich SW, Arbuckle BE, Cohen LR, Roberts M, Nesto RW. Diastolic abnormalities in young asymptomatic diabetic patients assessed by pulsed Doppler echocardiography. J Am Coll Cardiol 1988;12:114–20.
6. Vered A, Battler A, Segal P, et al. Exercise-induced left ventricular dysfunction in young men with asymptomatic diabetes mellitus (diabetic cardiomyopathy). Am J Cardiol 1984;54:633–7.
7. Langer A, Freeman MR, Josse RG, Armstrong PW. Metaiodobenzylguanidine imaging in diabetes mellitus: assessment of cardiac sympathetic denervation and its relation to autonomic dysfunction and silent myocardial ischemia. J Am Coll Cardiol 1995;25:610–8.
8. Stevens MJ, Raffel DM, Allman KC, et al. Cardiac sympathetic dysinnervation in diabetes: an explanation for enhanced cardiovascular risk? Circulation 1998;98:961–8.
9. Stevens MJ, Dayanikli F, Raffel DM, et al. Scintigraphic assessment of regionalized defects in myocardial sympathetic innervation and blood flow regulation in diabetic patients with autonomic neuropathy. J Am Coll Cardiol 1998;31:1575–84.
10. Nabel EG, Ganz P, Gordon JB, Alexander RW, Selwyn AP. Dilation of normal and constriction of atherosclerotic coronary arteries caused by the cold pressor test. Circulation 1988;77:43–52.
11. Nitenberg A, Valensi P, Sachs R, Dali M, Aptecar E, Attali JR. Impairment of coronary vascular reserve and ACh-induced coronary vasodilation in diabetic patients with angiographically normal coronary arteries and normal left ventricular systolic function. Diabetes 1993;42:1017–25.
12. Di Carli MF, Janisse J, Grunberger G, Ager J. Role of chronic hyperglycemia in the pathogenesis of coronary microvascular dysfunction in diabetes. J Am Coll Cardiol 2003;41:1387–93.
13. Pitkanen OP, Nuutila P, Raitakari OT, et al. Coronary flow reserve is reduced in young men with IDDM. Diabetes 1998;47:248–54.
14. Di Carli MF, Bianco-Batlles D, Landa ME, et al. Effects of autonomic neuropathy on coronary blood flow in patients with diabetes mellitus. Circulation 1999;100:813–9.
15. Paulson DJ, Light KE. Elevation of serum and ventricular norepinephrine content in the diabetic rat. Res Commun Chem Pathol Pharmacol 1981;33:559–62.
16. Schmid H, Forman LA, Cao X, Sherman PS, Stevens MJ. Heterogeneous cardiac sympathetic denervation and decreased myocardial nerve growth factor in streptozotocin-induced diabetic rats: implications for cardiac sympathetic dysinnervation complicating diabetes. Diabetes 1999;48:603–8.
17. Givertz MM, Sawyer DB, Colucci WS. Antioxidants and myocardial contractility: illuminating the "Dark Side" of beta-adrenergic receptor activation? Circulation 2001;103:782–3.
18. Felten SY, Peterson RG, Shea PA, Besch HR Jr., Felten DL. Effects of streptozotocin diabetes on the noradrenergic innervation of the rat heart: a longitudinal histofluorescence and neurochemical study. Brain Res Bull 1982;8:593–607.
19. Early Treatment Diabetic Retinopathy Study Research Group. Grading diabetic retinopathy from stereoscopic color fundus photo-

graphs—an extension of the modified Airlie House classification. ETDRS report number 10. Ophthalmology 1991;98:786–806.

20. American Diabetes Association. Diabetic nephropathy. Clinical practice recommendations. Diabetes Care 2002;25:S85–9.

21. Ewing DJ, Clarke BF. Diagnosis and management of diabetic autonomic neuropathy. Br Med J (Clin Res Ed) 1982;285:916–8.

22. Feldman EL, Stevens MJ, Thomas PK, Brown MB, Canal N, Greene DA. A practical two-step quantitative clinical and electrophysiological assessment for the diagnosis and staging of diabetic neuropathy. Diabetes Care 1994;17:1281–9.

23. Hutchins GD, Schwaiger M, Rosenspire KC, Krivokapich J, Schelbert H, Kuhl DE. Noninvasive quantification of regional blood flow in the human heart using N-13 ammonia and dynamic positron emission tomographic imaging. J Am Coll Cardiol 1990;15:1032–42.

24. Heath ME, Downey JA. The cold face test (diving reflex) in clinical autonomic assessment: methodological considerations and repeatability of responses. Clin Sci (Lond) 1990;78:139–47.

25. Garcia MJ, Thomas JD, Klein AL. New Doppler echocardiographic applications for the study of diastolic function. J Am Coll Cardiol 1998;32:865–75.

26. Ceriello A, Bortolotti N, Falleti E, et al. Total radical-trapping antioxidant parameter in NIDDM patients. Diabetes Care 1997;20:194–7.

27. Schnell O, Muhr D, Weiss M, Dresel S, Haslbeck M, Standl E. Reduced myocardial 123I-metaiodobenzylguanidine uptake in newly diagnosed IDDM patients. Diabetes 1996;45:801–5.

28. Stevens MJ, Raffel DM, Allman KC, Schwaiger M, Wieland DM. Regression and progression of cardiac sympathetic dysinnervation complicating diabetes: an assessment by C-11 hydroxyephedrine and positron emission tomography. Metabolism 1999;48:92–101.

29. DeGrado TR, Hutchins GD, Toorongian SA, Wieland DM, Schwaiger M. Myocardial kinetics of carbon-11-meta-hydroxyephedrine: retention mechanisms and effects of norepinephrine. J Nucl Med 1993;34:1287–93.

30. Nakajo M, Shapiro B, Glowniak J, Sisson JC, Beierwaltes WH. Inverse relationship between cardiac accumulation of meta-[131I]iodobenzylguanidine (I-131 MIBG) and circulating catecholamines in suspected pheochromocytoma. J Nucl Med 1983;24:1127–34.

31. Gasnier B, Roisin MP, Scherman D, Coornaert S, Desplanches G, Henry JP. Uptake of meta-iodobenzylguanidine by bovine chromaffin granule membranes. Mol Pharmacol 1986;29:275–80.

32. Thiene G, Nava A, Corrado D, Rossi L, Pennelli N. Right ventricular cardiomyopathy and sudden death in young people. N Engl J Med 1988;318:129–33.

33. Shindo H, Thomas TP, Larkin DD, et al. Modulation of basal nitric oxide-dependent cyclic-GMP production by ambient glucose, myo-inositol, and protein kinase C in SH-SY5Y human neuroblastoma cells. J Clin Invest 1996;97:736–45.

34. Vanhoutte PM, Miller VM. Alpha 2-adrenoceptors and endothelium-derived relaxing factor. Am J Med 1989;87:1–5S.

35. Hogikyan RV, Galecki AT, Halter JB, Supiano MA. Heightened norepinephrine-mediated vasoconstriction in type 2 diabetes. Metabolism 1999;48:1536–41.

36. Wu QD, Wang JH, Fennessy F, Redmond HP, Bouchier-Hayes D. Taurine prevents high-glucose-induced human vascular endothelial cell apoptosis. Am J Physiol 1999;277:C1229–38.

37. Ludmer PL, Selwyn AP, Shook TL, et al. Paradoxical vasoconstriction induced by acetylcholine in atherosclerotic coronary arteries. N Engl J Med 1986;315:1046–51.

38. Yokoyama I, Ohtake T, Momomura S, et al. Hyperglycemia rather than insulin resistance is related to reduced coronary flow reserve in NIDDM. Diabetes 1998;47:119–24.

39. Torry RJ, Connell PM, O'Brien DM, Chilian WM, Tomanek RJ. Sympathectomy stimulates capillary but not precapillary growth in hypertrophic hearts. Am J Physiol 1991;260:H1515–21.

40. Whall CW Jr., Myers MM, Halpern W. Norepinephrine sensitivity, tension development and neuronal uptake in resistance arteries from spontaneously hypertensive and normotensive rats. Blood Vessels 1980;17:1–15.

41. Communal C, Singh K, Pimentel DR, Colucci WS. Norepinephrine stimulates apoptosis in adult rat ventricular myocytes by activation of the beta-adrenergic pathway. Circulation 1998;98:1329–34.

42. Gambardella S, Frontoni S, Spallone V, et al. Increased left ventricular mass in normotensive diabetic patients with autonomic neuropathy. Am J Hypertens 1993;6:97–102.